

## Phase Transformations of 1.4 at % Cu–Al Binary Alloy at High Pressures and Temperatures

A. G. Padalko<sup>a, \*</sup>, T. K. Akopyan<sup>a</sup>, M. S. Pyrov<sup>a</sup>, A. D. Izotov<sup>b</sup>, A. V. Khoroshilov<sup>b</sup>, and G. V. Talanova<sup>a</sup>

<sup>a</sup>*Baikov Institute of Metallurgy and Materials Science, Russian Academy of Sciences, Leninskii pr. 49, Moscow, 119991 Russia*

<sup>b</sup>*Kurnakov Institute of General and Inorganic Chemistry, Russian Academy of Sciences, Leninskii pr. 31, Moscow, 119991 Russia*

\**e-mail: padalko@inbox.ru*

Received February 15, 2019; revised April 19, 2019; accepted April 22, 2019

**Abstract**—Phase transformations of 1.4 at % Cu + 98.6 at % Al alloy have been studied at atmospheric pressure by differential scanning calorimetry and at a moderately high hydrostatic pressure (~100 MPa) by differential barothermal analysis. High pressure has been shown to raise the solvus ( $\theta$ -Al<sub>2</sub>Cu +  $\alpha$ -Al →  $\alpha$ -(Al) solid-state transformation) temperature of the alloy relative to the equilibrium value obtained at atmospheric pressure. According to our estimate, the heat of solid-state  $\theta$ -phase dissolution in the  $\alpha$ -matrix at 100 MPa is four times that at atmospheric pressure. High-pressure crystallization has been shown to have a significant effect on the microstructure of the alloy, with a manyfold increase in the particle size of the  $\theta$ -Al<sub>2</sub>Cu intermetallic phase.

**Keywords:** binary alloy, pressure, temperature, phase transformation, liquidus, solidus, solvus

**DOI:** 10.1134/S0020168519090115

### INTRODUCTION

Copper-containing aluminum alloys constitute the most widespread group of aluminum alloys. In particular, there are 14 domestically produced copper silumins, which contain 5–21 wt % silicon and 1–7 wt % copper (AK5M, AK5Mch, and others) [1]. Like in the case of essentially all metallic materials, the manufacture of aluminum alloys relies on the use of canonical binary phase equilibrium diagrams, Al–Si and Al–Cu in the case under consideration [2, 3], which were constructed using results of numerous experiments, including thermoanalytical ones carried out at atmospheric pressure.

In the composition range 0–53 wt % Cu, the Al–Cu binary system has eutectic phase relations:  $\alpha$ -Al +  $\theta$ -CuAl<sub>2</sub>. The highest copper solubility in the aluminum-based  $\alpha$ -solid solution (at the eutectic temperature, 548°C) is 5.7 wt %. With decreasing temperature, copper solubility decreases, down to 0.5 wt % at 300°C. Note that reliable data on solid-state solubility of Al<sub>2</sub>Cu in an  $\alpha$ -matrix containing ≤5.7 wt % copper are crucial for the ability to control the properties of copper-containing silumins via heat treatment. In this case,  $\theta$ -phase dissolution during heating and subsequent precipitation of metastable copper-containing compounds upon the decomposition of a supersaturated Al-based solid solution allow the mechanical properties of copper silumins to be controlled to a significant degree. The use of pressure during heat treat-

ment of copper-containing aluminum alloys requires reliable data on their characteristic temperatures at elevated pressures.

The purpose of this work is to study phase transformations, including solid-state ones, in the Al–Cu binary system, which is currently of great practical interest given the wide use of hot isostatic pressing (barothermal processing) in modern materials engineering [4].

### EXPERIMENTAL

The subject of this study was an alloy containing 1.4 at % copper, with an (Al) + Al<sub>2</sub>Cu → (Al) transition at 478°C, a solidus temperature of 599°C, and a liquidus temperature of 653°C according to equilibrium phase diagram data [2, 3]. The 1.4 at % Cu + 98.6 at % Al (1.4Cu–Al) alloy was synthesized in a laboratory-scale electric resistance furnace via melting of A99 Al (99.99%) and M1 Cu (99.9%) in graphite–chamotte crucibles at a temperature of 750°C for 2 h. The melt was cast into a graphite mold at a melt temperature in the range 730–750°C. In this way, we obtained ingots with a rectangular cross section, 20 × 10 × 150 mm in dimensions.

Thermal analysis was carried out at atmospheric pressure using differential scanning calorimetry (DSC) in an STA 449F1 Jupiter simultaneous thermal analysis system (Netzsch, Germany) under an argon

atmosphere (5.5 grade, 99.9995%). First, the instrument was calibrated in terms of temperature and sensitivity using metallic standards. As a result, the uncertainty in our temperature measurements was no greater than  $\pm 0.3^\circ\text{C}$ , and sensitivity was determined with an accuracy of  $\pm 3\%$ . DSC scans were carried out in lidded alundum crucibles. The type of measurement was a sample with correction. The measurements were performed at a heating/cooling rate of  $7^\circ\text{C}/\text{min}$ . The heat of phase transformations was calculated with Netzsch-Proteus-Thermal Analysis version 5.2.1 software. The solvus, solidus, and liquidus temperatures extracted from equilibrium phase diagram data [2, 3] and the DSC curves obtained at 0.1 MPa were taken to be references in interpreting differential barothermal analysis curves.

Thermal events at an argon pressure of 100 MPa were recorded using a differential thermal analysis cell placed in a high-pressure vessel of a hot isostatic pressing system (ABRA, Switzerland) [5–9] at the same heating/cooling rate as in DSC:  $7^\circ\text{C}/\text{min}$ . In microstructural analysis, we used an MeF3 optical microscope (Austria) equipped with an accessory for obtaining digital images. X-ray diffraction patterns were collected on an XRD-6000 diffractometer (Shimadzu, Japan) with nickel-filtered  $\text{Cu}K_\alpha$  radiation. To improve microstructure imaging quality and obtain quantitative information about the structural constituents of the alloy, we used Adobe Photoshop CS6 and ImageJ software. In experimental data processing, we used the Origin 5.0 program.

## RESULTS AND DISCUSSION

In the as-synthesized, unhomogenized cast samples in the initial state, the intermetallic  $\theta$ -phase was evenly distributed over the aluminum matrix, without well-defined grain boundaries in primary aluminum crystals. The  $\text{Al}_2\text{Cu}$  particles were rounded in shape, with small agglomerates formed by two to seven particles (Fig. 1). Images obtained on an optical microscope were analyzed using Adobe Photoshop CS6 and ImageJ. As a result, we obtained the size distribution of the intermetallic particles in Fig. 1c. The distribution is well represented by an exponential of the form

$$N_{\text{Al}_2\text{Cu}}^0 = 1.4 \times 10^2 e^{-0.53d_{\text{eq}}}, \quad (1)$$

where  $N_{\text{Al}_2\text{Cu}}^0$  is the number of  $\text{Al}_2\text{Cu}$  particles in the image of the as-prepared alloy and  $d_{\text{eq}}$  ( $\mu\text{m}$ ) is the equivalent particle diameter. The quantitative characteristics of the  $\theta$ -phase are summarized in Table 1.

The obtained volume number density of intermetallic particles is well consistent with the copper content of the alloy. Such results are characteristic of microstructure formation in the alloy containing 1.4 at % copper, which falls in the solid solution range. In this case, cooling the alloy that rapidly crystallized when cast into a mold is accompanied by nonequilibrium

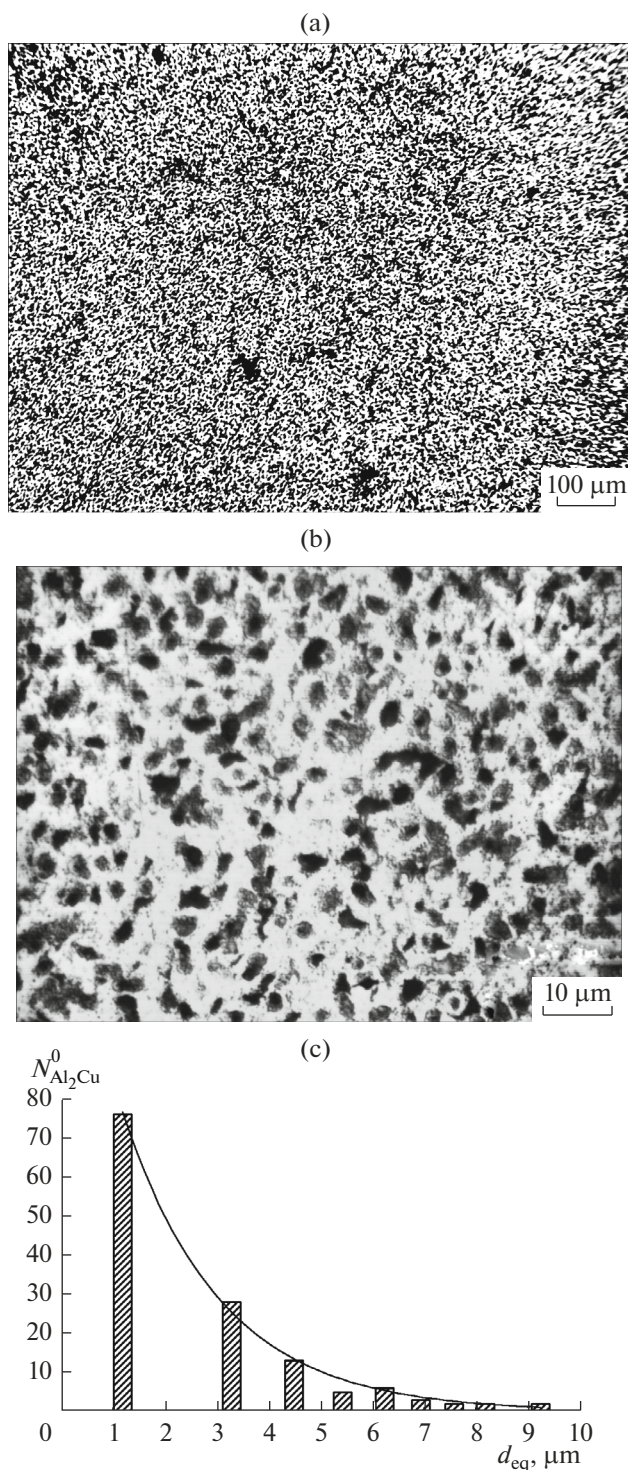


**Fig. 1.** (a) Microstructure of the 1.4Cu–Al as-synthesized alloy; (b) optical micrograph and (c) size distribution of the  $\text{Al}_2\text{Cu}$  particles in the aluminum matrix of the as-synthesized alloy.

crystallization of the binary eutectic,  $L \rightarrow (\text{Al}) + \text{Al}_2\text{Cu}$ , resulting in the formation of the nonequilibrium  $\theta$ -phase in the structure of the alloy. The particles of this phase are evenly distributed along dendritic

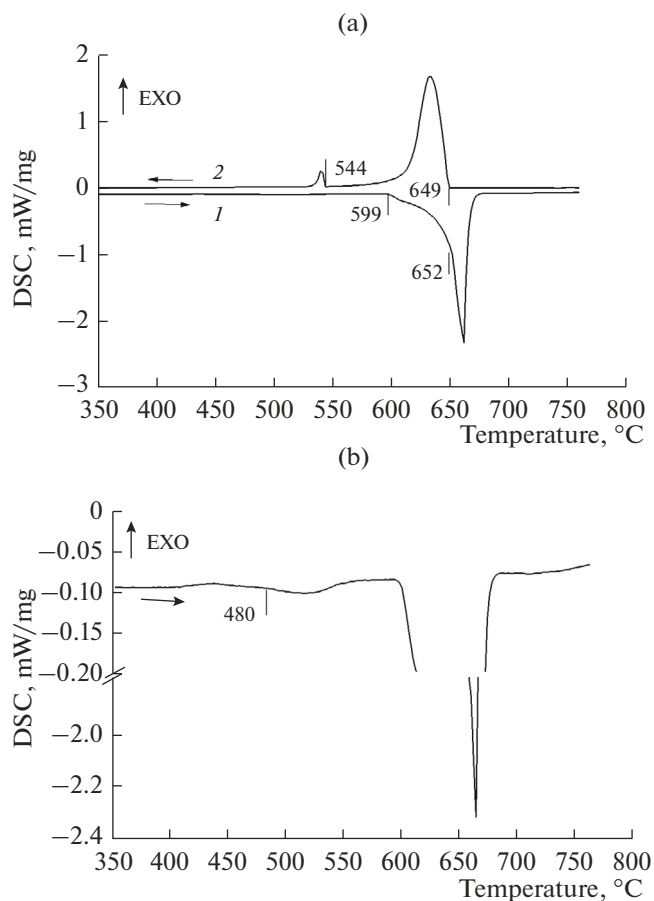
**Table 1.** Quantitative characteristics of Al<sub>2</sub>Cu intermetallic particles according to data processing with ImageJ

Image	Number of Al <sub>2</sub> Cu particles in the image	Average particle diameter, cm	Average particle volume, cm <sup>3</sup>	Volume number density of particles, cm <sup>-3</sup>
As-prepared alloy (Fig. 1b), 1.0 < d <sub>Al<sub>2</sub>Cu</sub> < 10 μm	137	3.9 × 10 <sup>-4</sup>	3.1 × 10 <sup>-11</sup>	4.2 × 10 <sup>9</sup>
Alloy after a DBA cycle (Fig. 5a), 5.0 < d <sub>Al<sub>2</sub>Cu</sub> < 150 μm	127	5.9 × 10 <sup>-3</sup>	1.1 × 10 <sup>-7</sup>	5.4 × 10 <sup>5</sup>

cells of the slightly doped aluminum-based solid solution (Al).

From the as-cast ingot, we cut samples for characterization by DSC at atmospheric pressure of high-purity argon and differential barothermal analysis (DBA). Reference DSC curves obtained at an argon pressure of 0.1 MPa are shown in Fig. 2.

From the DSC heating curve (Fig. 2a, curve 1), the solidus temperature was determined to be 599°C, and the liquidus temperature, 651°C. From the cooling



**Fig. 2.** (a) DSC curves of the 1.4Cu–Al alloy at atmospheric pressure: (1) heating, (2) cooling; (b) DSC heating curve presented with a discontinuous vertical axis.

curve (curve 2), the liquidus temperature was determined to be 649°C (which coincides with the equilibrium value), and the crystallization temperature of the nonequilibrium eutectic, 544°C. The solidus temperature evaluated from the heating curve slightly exceeds that in the equilibrium Al–Cu phase diagram [2, 3]. This circumstance is most likely due to the non-equilibrium conditions of our DSC experiments, which shifted the melting onset of the alloy to higher temperatures. It follows from the present experimental data that, in the DSC heating and cooling curves presented with standard heat of transformation and temperature (time) axes, it is essentially impossible to determine the solvus temperature (solid-state dissolution of the intermetallic particles) (Fig. 2a). At the same time, presenting the curves with a discontinuous vertical (heat of transformation) axis makes it possible to obtain a heating curve (Fig. 2b) suitable for evaluating the dissolution temperature of the intermetallic phase at atmospheric pressure (0.1 MPa). From the DSC heating curve, taking into account the solvus temperature [2, 3], we find that the dissolution of the Al<sub>2</sub>Cu particles begins at 480°C. Note that the endothermic peak of the solid → solid transformation (dissolution of the θ-phase) in the DSC heating curve indicates that the solid-state transformation has a rather small heat effect. In our DSC experiments, we determined the heat of fusion (solid → liquid transformation) of the 1.4Cu–Al alloy using standard software supplied with the Netzsch STA 449F1 Jupiter: 329.5 J/g. To find the small heat of the solid → solid transformation (dissolution of the θ-phase), we used the capabilities of Netzsch-Proteus-Thermal Analysis software. For this purpose, a portion of the DSC heating curve in the temperature range 430–545°C was analyzed separately. According to our calculations, the heat of the α-(Al) + θ-Al<sub>2</sub>Cu → (Al) transformation at 0.1 MPa is 7.67 J/g (2.3% of the heat of the solid → liquid transformation).

To assess the capabilities of Origin software, we utilized a similar approach for evaluating the heat effect of the same transformation using the experimental data obtained with a reference DSC curve. Integrating the weak endothermic peak yielded ~7.7 J/g, in excellent agreement with the heat of transformation

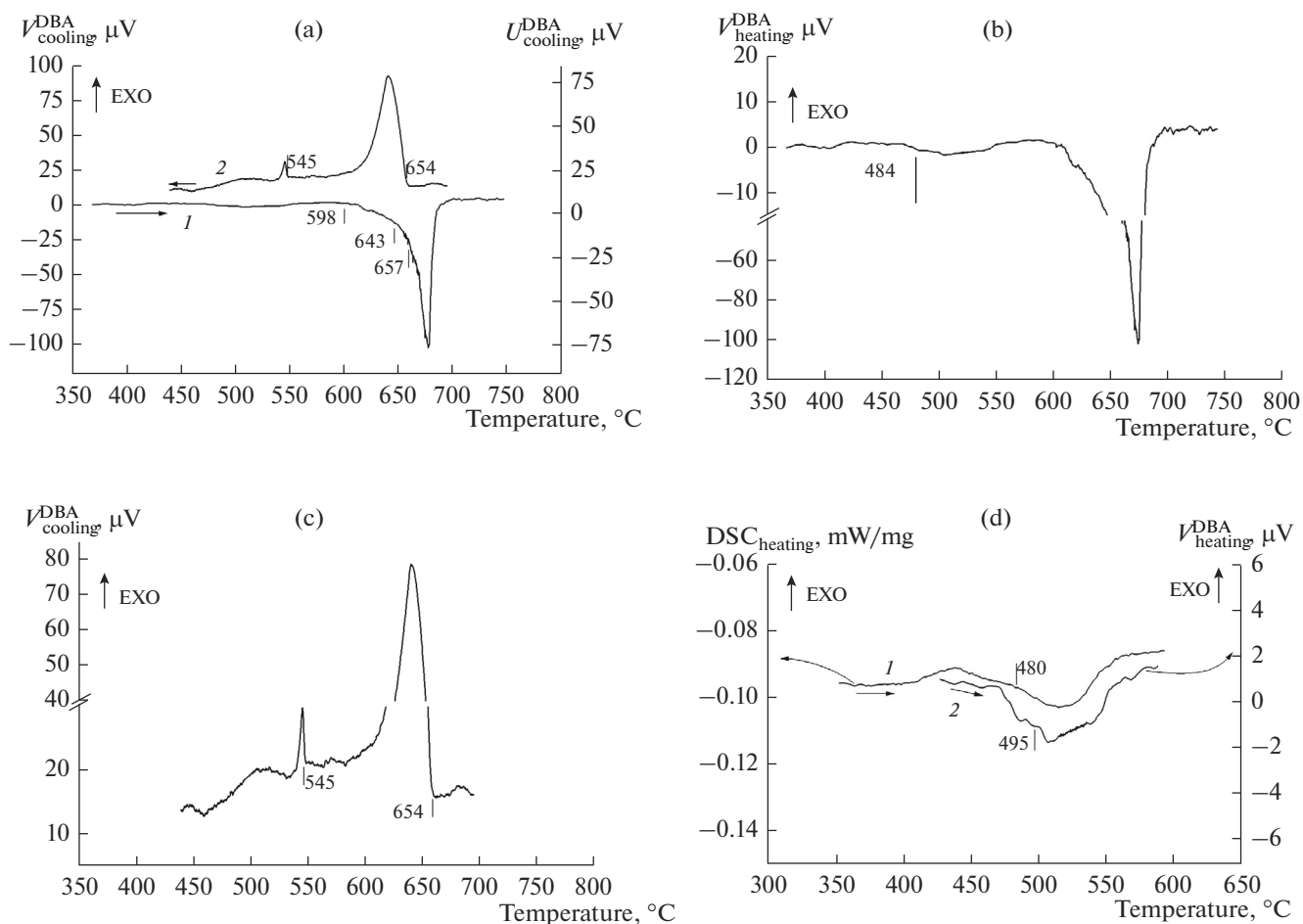


**Fig. 3.** (a) DBA (1) heating and (2) cooling curves of the 1.4Cu–Al binary alloy at a pressure of 100 MPa; (b) curve 1 presented with a discontinuous vertical axis; (c) curve 2 presented with a discontinuous vertical axis; (d) portions of the (1) DSC and (2) DBA heating curves used to determine  $t_{\text{solvus}}$ .

obtained using Netzsch-Proteus-Thermal Analysis software.

In barothermal scans, we used samples of the as-prepared 1.4Cu–Al alloy 4 mm in diameter and 7 mm in length. A set of miniature molybdenum disks 4 mm in diameter and 0.5 mm in thickness, each weighing 20 mg, were used as a reference. The total weight of the reference coincided with the weight of the sample to within  $\pm 3$  mg. The measurements were performed in argon compressed to  $\sim 100$  MPa (near solid  $\rightarrow$  liquid (liquid  $\rightarrow$  solid) phase transformations) at a heating/cooling rate of  $7^\circ\text{C}/\text{min}$  (the same as in the DSC measurements under ordinary conditions). The DBA curves thus obtained are presented in Fig. 3. It is seen in the heating curve of the alloy (Figs. 3b, 3d) that the  $\theta$ -phase dissolution process begins at  $484^\circ\text{C}$ , that is,  $4^\circ\text{C}$  above the DSC results.

The liquidus temperature evaluated from the DBA cooling curve (Fig. 3c) is  $654^\circ\text{C}$  ( $5^\circ\text{C}$  above the DSC data and the equilibrium value [2, 3]). The crystallization temperature of the nonequilibrium eutectic

( $545^\circ\text{C}$ ) remained essentially unchanged relative to the DSC data and the equilibrium value. The DSC and DBA results are summarized in Table 2.

To evaluate the heat of the solid  $\rightarrow$  solid transformation at 100 MPa, we used the approach described above in analyzing the DSC heating curve. In doing so, we assumed the heat effect of fusion of the alloy at a pressure of 100 MPa to be close to that determined by DSC:  $329.5$  J/g. From the DBA heating curve, the ratio of the areas of the endothermic peak due to the dissolution of the  $\theta$ -phase in the  $\alpha$ -matrix,  $\alpha\text{-(Al)} + \theta\text{-CuAl}_2 \rightarrow \alpha\text{-(Al)}$ , in the range  $470\text{--}580^\circ\text{C}$  and the endothermic peak due to the melting of the alloy,  $(\text{Al})_s \rightarrow \text{Al}_l$ , in the range  $583\text{--}700^\circ\text{C}$  was determined to be 8.5%. With allowance for the above assumptions, the corresponding heat effect of the transformation at moderate pressures is  $\sim 28$  J/g.

The relatively small heat effects of the dissolution/precipitation of the  $\theta$ -phase correlate with the small heats of precipitation of silicon particles from the aluminum-based solid solution in Al–0.72Si and

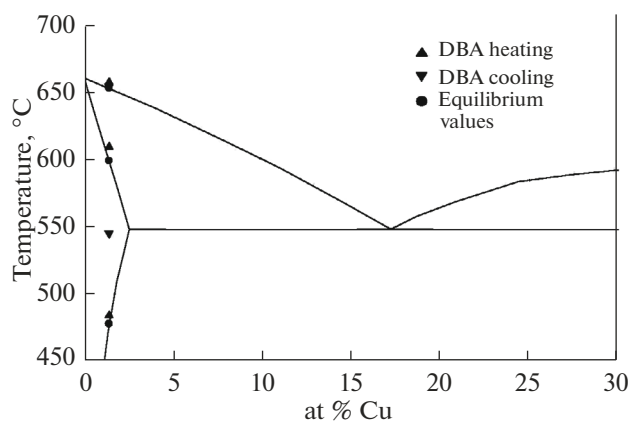
**Table 2.** Temperatures (°C) of phase transformations of the 1.4Cu–Al alloy as determined by DSC (at 0.1 MPa) and DBA (at 100 MPa) in comparison with equilibrium values

Method	$t_{\text{solvus}}$		$t_S$		$t_L$		$t'_{\text{eut}}$	
	I	II	I	II	I	II	I	II
From the equilibrium phase diagram [1, 2]	478		599		653		$t_{\text{eut}}^{\text{eq}} = 548$	
DSC	480	–	599	–	652	649	–	544
DBA	484	–	609	–	657	654	–	545

I, heating; II, cooling.

Al–0.26Si binary alloys, which were studied at slow cooling rates (down to 0.001 K/s). In that case, the amplitude of the heat effects of solid-state silicon precipitation was within 0.17 and 0.05 J/(g K), respectively [10]. The considerable increase in the heat of dissolution at 100 MPa in comparison with the heat effect of this transformation at atmospheric pressure is due to the pressure factor, which probably leads to an increase in the activation energy for copper diffusion in the alloy under study. Thus, according to the DSC data obtained at 0.1 MPa, the heat effects of the transformations of the 1.4Cu–Al alloy were 329.5 J/g for the solid → liquid transition (melting) and 7.7 J/g for the solid → solid transformation. At the same time, according to estimates based on the DBA data obtained at ~100 MPa, the heat effect of the solid → solid transformation was 28 J/g.

The DBA data were compared to the equilibrium Al–Cu phase diagram (Fig. 4). An applied pressure was shown to have the weakest effect on the liquidus and nonequilibrium eutectic crystallization tempera-

**Fig. 4.** Partial equilibrium Al–Cu phase diagram with data points obtained by DBA.

tures. The pressure-induced shift of the solidus and solvus temperatures is more pronounced and should be taken into account in performing barothermal processing (hot isostatic pressing) of copper-containing aluminum alloys.

After crystallization in a DBA cell at 100 MPa, the alloy had a markedly coarser microstructure, with a considerable increase in the size of both primary aluminum and Al<sub>2</sub>Cu intermetallic crystals (Fig. 5). Analyzing the image in Fig. 5a, we obtained a particle size distribution of the  $\theta$ -phase, presented in Fig. 5b. The distribution is well represented by an exponential of the form

$$N_{\text{Al}_2\text{Cu}}^{\text{DBA}} = 2.1 \times 10^2 e^{-0.04d_{\text{eq}}}, \quad (2)$$

where  $N_{\text{Al}_2\text{Cu}}^{\text{DBA}}$  is the number of Al<sub>2</sub>Cu particles in the alloy after DBA and  $d_{\text{eq}}$  ( $\mu\text{m}$ ) is the equivalent particle diameter. According to data processing with ImageJ, the number of Al<sub>2</sub>Cu intermetallic particles in the image in the range  $d_{\text{Al}_2\text{Cu}} = 5.0\text{--}150 \mu\text{m}$  was ~127, the average particle diameter was  $5.9 \times 10^{-3} \text{ cm}$ , the average particle volume was  $1.1 \times 10^{-7} \text{ cm}^3$ , and the volume number density of particles was  $5.4 \times 10^5 \text{ cm}^{-3}$  (Table 1).

It follows from comparison of quantitative characteristics of the  $\theta$ -phase (Table 1) formed in the as-prepared material and after high-pressure crystallization that they undergo considerable changes. In particular, the average equivalent particle diameter increases by 15 times, the particle volume increases by three orders of magnitude, and the number density of particles drops by four orders of magnitude. The quantitative characteristics of the  $\theta$ -phase lead us to conclude that an applied pressure has no significant effect on the alloy solidification process, which takes place at insignificant supercooling, zero temperature gradient in the melt, and a low cooling rate. These parameters are determined by the thermal analysis conditions in our

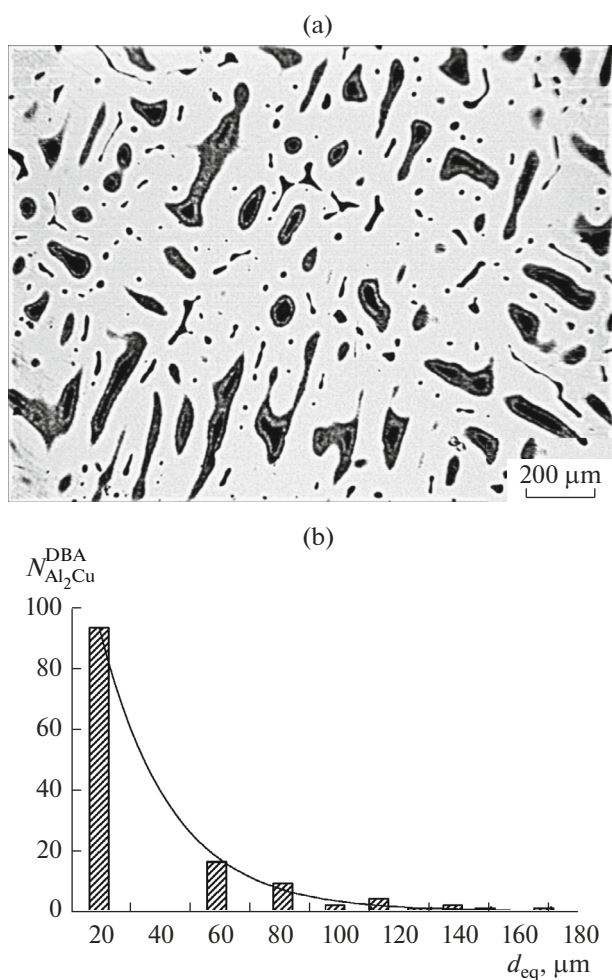


**Fig. 5.** (a) Microstructure of the 1.4Cu–Al alloy after a DBA cycle at 100 MPa; (b) size distribution of the  $\text{Al}_2\text{Cu}$  particles.

experiments and are responsible for the increase in the size of the structural constituents of the alloy.

The lattice parameters and phase composition of the 1.4Cu–Al alloy after a DBA cycle were determined by X-ray diffraction using a ground sample (Fig. 6). Its X-ray diffraction pattern contained only reflections from (Al) and the  $\theta$ -phase. To find the lattice parameter of the aluminum-based solid solution after high-pressure melting and crystallization, the Al 111 and 200 peaks were decomposed into their  $\text{CuK}_{\alpha 1}$  and  $\text{CuK}_{\alpha 2}$  components. The value thus obtained,  $a_{\text{Al}}^{\text{DBA}} = 4.048 \text{ \AA}$ , is smaller than the reference value  $a_{\text{Al}}^{\text{ref}} = 4.049 \text{ \AA}$ . The observed decrease in lattice parameter is due to the formation of an aluminum-based solid solution containing copper atoms inserted in its lattice, which is a thermodynamically promoted process accompanied by a reduction in the specific volume of the  $\alpha$ -matrix upon the formation of a solid solution at high pressures. The reduction in lattice parameter during fast nonequilibrium cooling of ribbons of Al–Cu binary alloys was also attributed by Lichioiu et al. [11] to copper dissolution in the aluminum lattice.

## CONCLUSIONS

The solvus (solid-state transformation) temperature of the 1.4Cu–Al alloy at 100 MPa exceeds equilibrium values and DSC results obtained at atmospheric pressure. According to our estimate, the heat of solid-state  $\theta$ -phase dissolution in the  $\alpha$ -matrix is a factor of  $\sim 3.7$  larger than that at atmospheric pressure. The solidus temperature of the alloy at 100 MPa exceeds that determined by DSC at 0.1 MPa by  $10^\circ\text{C}$ , and the liquidus temperature increases by  $5\text{--}6^\circ\text{C}$ . Melting and crystallization at 100 MPa increase the size of the structural constituents of the alloy by many times,

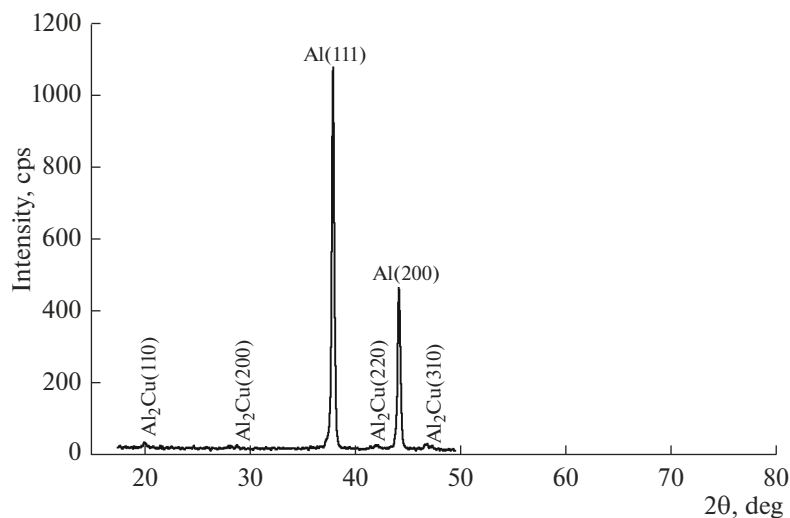


**Fig. 6.** X-ray diffraction pattern of a  $\text{CuAl}_2$  powder sample after DBA.

which is determined primarily by the thermophysical parameters of the solidification process in a DBA cell.

#### FUNDING

This work was supported by the Russian Federation Ministry of Science and Higher Education through the state research targets for the Baikov Institute of Metallurgy and Materials Science, Russian Academy of Sciences (theme no. 007-00129-18-00) and the Kurnakov Institute of General and Inorganic Chemistry, Russian Academy of Sciences (theme no. 01201353364) in the field of basic research.

#### REFERENCES

1. Prigunov, A.G., Belov, N.A., Taran, Yu.N., Zolotarevskii, V.S., Napalkov, V.I., and Petrov, S.S., *Siluminy. Atlas mikrostruktur i fraktogramm promyshlennykh splavov* (Silumins: Atlas of Microstructures and Fracture Surface Maps for Industrial Alloys), Moscow: Mosk. Inst. Stali i Splavov, 1996.
2. *Diagrammy sostoyaniya dvoinykh metallicheskih sistem* (Phase Diagrams of Binary Metallic Systems), 3 vols., Lyakishev, N.P., Ed., Moscow: Mashinostroenie, 1996, 1997, 2001.
3. Hansen, M. and Anderko, K., *Constitution of Binary Alloys*, New York: McGraw-Hill, 1958, 2nd ed., vols. 1–2.
4. Padalko, A.G., *Praktika goryachego izostaticheskogo pressovaniya neorganicheskikh materialov* (Practical Issues in Hot Isostatic Pressing of Inorganic Materials), Moscow: Akademkniga, 2007.
5. Padalko, A.G., Veselov, A.N., Avduhin, S.P., et al., Differential barothermal analysis (DBA) of Ni-base alloys, *J. Therm. Anal. Calorim.*, 2003, vol. 72, no. 3, pp. 791–797.  
<https://doi.org/10.1023/A:1025005912710>
6. Padalko, A.G., Belov, N.A., Veselov, A.N., and Talanova, G.V., Thermography of the phase transformations in a hypoeutectic Al–7% Si–0.5% Mg silumin at high pressures and temperatures, *Russ. Metall. (Engl. Transl.)*, 2009, no. 1, pp. 65–60.
7. Padalko, A.G., Talanova, G.V., Zubarev, G.I., Fedotov, V.T., Suchkov, A.N., and Tsarev, V.I., Thermography of the phase transformations in nickel-based eutectic alloys at high pressures and temperatures, *Russ. Metall. (Engl. Transl.)*, 2011, no. 3, 169–174.
8. Padalko, A.G., Talanova, G.V., Ponomareva, E.Yu., Talyat-Kelpsh, V.V., Shvorneva, L.I., Zubarev, G.I., Fedotov, V.T., Suchkov, A.N., and Baklan, V.A., Phase transformations at high pressures and temperatures and the structure of a hypoeutectic 1Ni–99Al alloy, *Russ. Metall. (Engl. Transl.)*, 2012, no. 9, pp. 779–785.
9. Padalko, A.G., Talanova, G.V., Ponomareva, E.Yu., Talyat-Kelpsh, V.V., Shvorneva, L.I., Zubarev, G.I., Fedotov, V.T., Suchkov, A.N., and Baklan, V.A., Barothermal analysis and structure of the eutectic Al–Ni (2.7 at % Ni) alloy, *Inorg. Mater.*, 2012, vol. 48, no. 6, pp. 582–587.
10. Schumacher, P., Pogatscher, S., Starink, M.J., Schick, C., Mohles, V., and Milkereit, B., Quench-induced precipitates in Al–Si alloys: calorimetric determination of solute content and characterization of microstructure, *Thermochim. Acta*, 2015, vol. 602, pp. 63–73.  
<https://doi.org/10.1016/j.tca.2014.12.023>
11. Lichioiu, I., Peter, I., Varga, B., and Rosso, M., Preparation and structural characterization of rapidly solidified Al–Cu alloys, *J. Mater. Sci. Technol.*, 2014, vol. 30, no. 4, pp. 394–400.  
<https://doi.org/10.1016/j.jmst.2013.12.001>

Translated by O. Tsarev